**Liquid Crystals**
Publication details, including instructions for authors and subscription information:
http://www.informaworld.com/smpp/title~content=t713926090

# Ordered structure of thermotropic liquid crystalline copolymers 2. Observation of annihilation kinetics of wedge disclinations

Toshio Shiwaku[ab]; Akemi Nakai[ac]; Wei Wang[a]; Hirokazu Hasegawa[a]; Takeji Hashimoto[a]
[a] Department of Polymer Chemistry, Graduate School of Engineering, Kyoto University, Kyoto, Japan [b] Polyplastics Co., Ltd, Research Center, Japan [c] Department of the Home Economics, Kyushu Women's Junior College, Kitakyushu, Japan

**To cite this Article** Shiwaku, Toshio , Nakai, Akemi , Wang, Wei , Hasegawa, Hirokazu and Hashimoto, Takeji(1995) 'Ordered structure of thermotropic liquid crystalline copolymers 2. Observation of annihilation kinetics of wedge disclinations', Liquid Crystals, 19: 5, 679 — 691

**To link to this Article: DOI:** 10.1080/02678299508031084

**URL:** http://dx.doi.org/10.1080/02678299508031084

LIQUID CRYSTALS, 1995, VOL. 19, NO. 5, 679–691

# Ordered structure of thermotropic liquid crystalline copolymers 2. Observation of annihilation kinetics of wedge disclinations

by TOSHIO SHIWAKU†, AKEMI NAKAI‡, WEI WANG,
HIROKAZU HASEGAWA and TAKEJI HASHIMOTO*
Department of Polymer Chemistry, Graduate School of Engineering,
Kyoto University, Kyoto 606-01, Japan

(*Received 23 December 1994; in final form 25 May 1995; accepted 2 June 1995*)

The isothermal annihilation kinetics of wedge disclinations in the fully liquid crystalline state were investigated using thin film specimens of a thermotropic liquid crystalline copolyester prepared by a solution-cast method. The as-cast films which are vitrified, homogeneous and amorphous were first subjected to a temperature jump to appropriate temperatures and the coarsening of the liquid crystalline texture was observed in real-time and *in situ* by means of optical microscopy and laser light scattering. The experimental results obtained show that, in the early stages, the domain size, $D$, which is inversely proportional to the square root of the density of disclinations in the sample, approximately obeys a power law of $D(t) \sim t^{0.35}$ over the time scale covered in the experiment. In the later stages, anchoring of some of the disclination lines onto the glass surface and/or formation of crystallites from some sequences of the copolyester having a higher melting point suppress and then pin the annihilation process. The annihilation processes for pairs of wedge disclinations between $s = +1/2$ and $s = -1/2$ or between $s = +1$ and $s = -1/2$ were directly observed *in situ* by optical microscopy, and the distance between them was observed to decrease with time.

## 1. Introduction

It is well known that the optical texture and properties of a liquid crystal (LC) sample are determined to a great extent by the type and the distribution of different kinds of defects [1–3]. For nematic liquids, the wedge disclinations with different strength and sign are primary defects. Interactions between two disclinations with opposite sign and their annihilation via diffusion-coalescence lead to a decrease in the number of disclinations and a coarsening of the schlieren texture. This is concerned with the dynamics of the ordering process by which an excess of free energy associated with the disclinations is released. The investigation of such an annihilation process is an important research item in the physics of liquid crystals. The annihilation process was first observed in a low molecular mass liquid crystal [4]. Recently such a process and its kinetics have been investigated experimentally for some low molecular mass liquid crystals and lyotropic or thermotropic liquid crystalline polymers by optical and electron microscopy, as well as by light scattering [5–13]. These experimental studies [4, 6, 8] further stimulated some theoretical [14, 15] and experimental [10, 11] explorations concerning the kinetics of annihilation of topological defects.

The copolyester studied comprised *p*-hydroxybenzoic acid (OBA) and ethylene terephthalate (PET) units in a 60/40 mol/mol composition and is one of the commercial thermotropic liquid crystalline polymers with a nematic nature [6–8, 16–19]. Its chemical structure is:

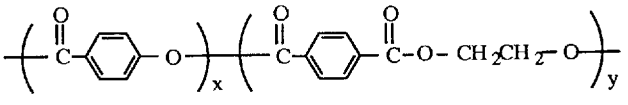

OBA 60 mol %
(Mesogenic seq.)

PET 40 mol %
(Flexible seq.)

The clearing temperature of this copolyester is higher than 400°C, close to its decomposition temperature [8]. Therefore it is difficult to erase a structure memory built into as-received or as-obtained polymer powder or pellets by a simple annealing at high temperatures. This fact usually makes it very difficult to compare the results reported in the literature on this copolyester when they were obtained from specimens prepared by hot-pressing,

---

* Author for correspondence.

† Present address: Polyplastics Co., Ltd, Research Center, 973 Miyajima, Fuji-city, Shizuoka-Pref. 416, Japan.

‡ Present address: Department of the Home Economics, Kyushu Women's Junior College, 1-1Jiyugaoka, Yawatanishi, Kitakyushu 807, Japan.

0267-8292/95 $10·00 © 1995 Taylor & Francis Ltd.

because of differences in the initial states and their memory effects on the texture at given temperatures.

In our previous studies we have characterized the liquid crystal domain texture [7, 8] and presented preliminary results on the annihilation kinetics of wedge disclinations [6] in film specimens of this copolyester. The thin film specimens were prepared by casting a homogeneous solution of the copolyester onto cover glasses. The as-cast films thus obtained were transparent, isotropic and glassy at room temperature. In this way we can erase the structure memory built into as-received polymers. The film preparation process is reproducible, and our results were also very reproducible indeed. In this study this preparation technique for thin film specimens was used again. Here we present the results obtained from a further extension of our studies of the annihilation process and kinetics of wedge disclinations in this thermotropic copolyester.

## 2. Experimental

The liquid crystalline polymer used is a statistical copolyester consisting of 60 mol % OBA and 40 mol % PET units with the trade name X-7G. Its number average molecular weight is *c.* $2 \times 10^4$. Test specimens were prepared in the same way as in previous studies [6–8] and we now briefly summarize the method below.

The as-received material in the form of pellets was dried at 60°C for 72 h and then dissolved in *o*-chlorophenol at a concentration of *c.* 2 wt % polymer at 60°C. The solution was carefully filtered, first using filter paper and subsequently a Millipore membrane with a pore size of 0·5 μm, in order to remove a small amount of fine insoluble particles which may be formed by the homopolymer of OBA or copolymers very rich in OBA units. One or two drops of this clear solution were put onto a microscope cover glass, and then the specimen was transferred into a vacuum oven preset at 60°C to evaporate the solvent as fast as possible. The solvent evaporation process took only a few minutes. The as-cast films with a thickness of a few micrometers were further dried under vacuum before they were used. The as-cast films prepared by this method were carefully checked by optical microscopy (OM) with or without crossed polarizers and wide angle X-ray scattering in order to make sure that the as-cast films were optically isotropic, amorphous and homogeneous. These as-cast films with one surface free (exposed to air) and the other surface on the microscope cover glass were used as the test specimens.

By means of a temperature jump method ($T$-jump), the test specimens were heated very fast to various temperatures by placing them on a heating stage (TH-600 Type, Linkam Scientific Co.) controlled at a preset temperature and sealed in $N_2$ gas atmosphere. Within one or two seconds, a liquid crystalline texture appeared in the film specimens. The texture was very fine in the beginning, because of the generation of a large number of topological defects (disclinations) during the rapid anisotropization process. The time-evolution of the liquid crystalline texture and the ordering processes due to annihilation of the defects were investigated by real-time and *in situ* observation using an optical microscope (Nikon Optiphot-Pol XTP-11) with or without crossed polarizers. When necessary, in order to freeze the texture of specimens during the ordering process, they were quenched to room temperature. The frozen specimens were further studied by optical microscopy and laser light scattering. In the laser light scattering experiment, a He–Ne laser source with a wavelength $\lambda_0 = 632{\cdot}8$ nm was used. The depolarized ($H_V$) scattering pattern could be obtained by setting vertical polarization for the incident beam and by observing the scattered light through a horizontally polarized analyser.

## 3. Results and discussion

### 3.1. *Kinetics of isothermal annihilation*

Our previous observations had shown that the solution-cast films form a pure nematic liquid crystalline phase in the temperature range between 180 and 370°C [8]. In the present study, we showed the test temperature in the range between 200 and 270°C, so avoiding the influence of complicated chemical reactions including transesterfication and decomposition at higher temperatures ( > 300°C) and crystallization of OBA or PET sequences in the lower temperature range ( < 200°C).

Figure 1 shows the optical texture of the X-7G thin film specimens obtained by isothermal annealing for 60 s at the various temperatures indicated in the figure. The micrographs on the left hand side of the figure were taken when using OM with crossed polarizers and show the typical schlieren texture of nematic liquid crystals as described in our previous study [6–8]. The orientation of the crossed polarizers is indicated by the letters A (analyser) and P (polarizer) in the figure. The micrographs on the right hand side of the figure were taken when using OM with only one polarizer and show clearly the location and the distribution of line or point disclinations which are indicated by the fine dark spots on the micrographs [6–8]. Under these conditions, we can directly identify the core of each disclination as a dark spot. The cores appear dark, because they strongly scatter light and hence do not transmit the incident light. With an increase of annealing temperature, the optimal texture at a given time after $T$-jump is coarsened, the number of disclinations decreases, and consequently the distance between the disclinations increases. These results indicate that the annihilation rate of disclinations increases with temperature over the temperature range covered in figure 1. Figure 2 shows the

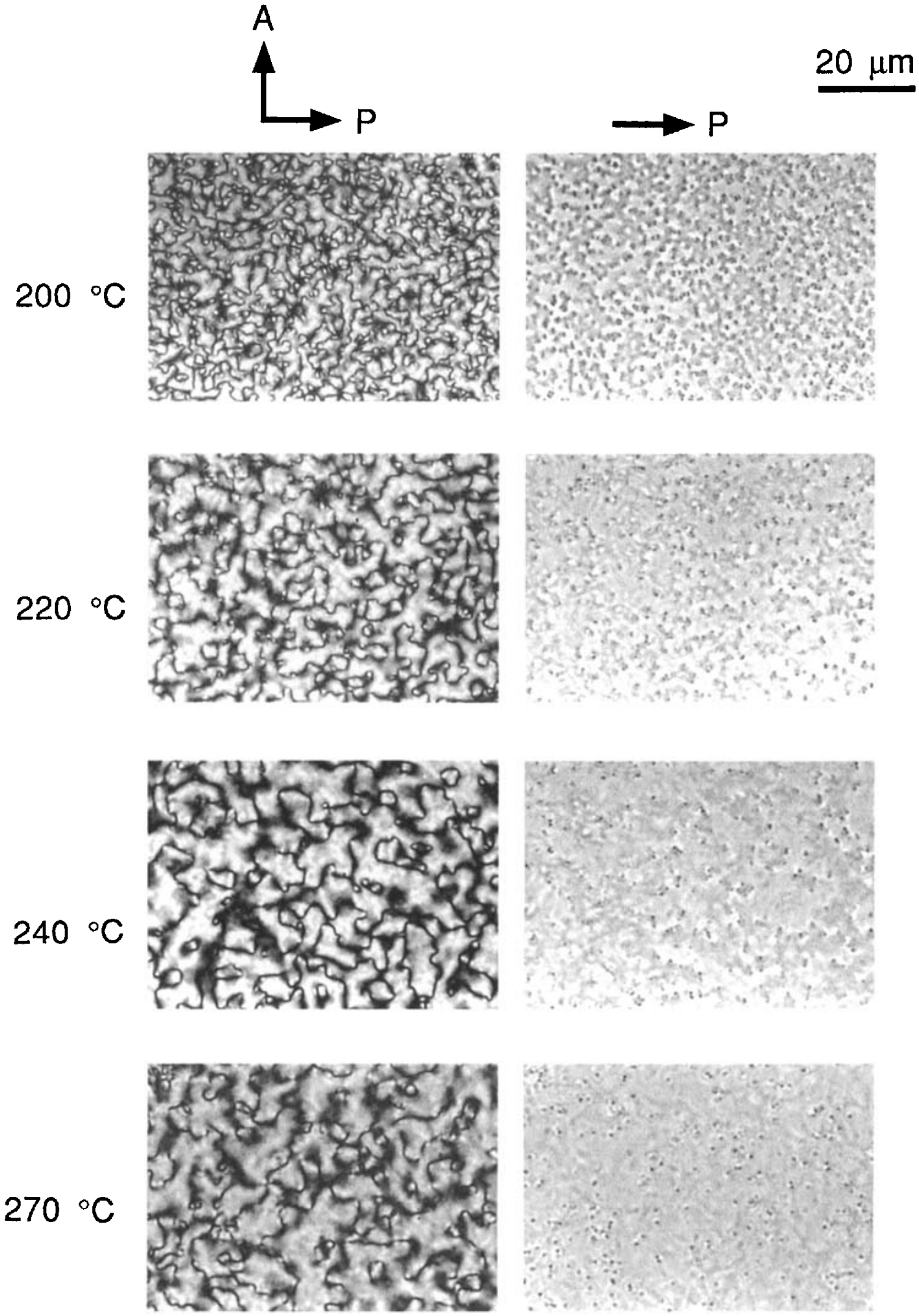

Figure 1. Variations of optical texture (left) and of the corresponding number of disclinations (right) with test temperature at 60 s. The polarizer and analyser are indicated by the letters P and A, respectively.

micrographs taken under the same conditions as for figure 1 and shows the time evolution of the ordering process at 240°C. It is clearly seen that coarsening of the texture and a decrease in the number density of disclinations occur with an increase in annealing time. The annihilation process will be discussed in detail in § 3.3.

The influence of the annealing temperature and time on the texture has also been investigated by the laser light scattering method, as shown in figure 3. The optical textures corresponding to some of these scattering patterns are shown in figure 1 or 2. The correlation between the scattering pattern and the spatial orientation distribution of

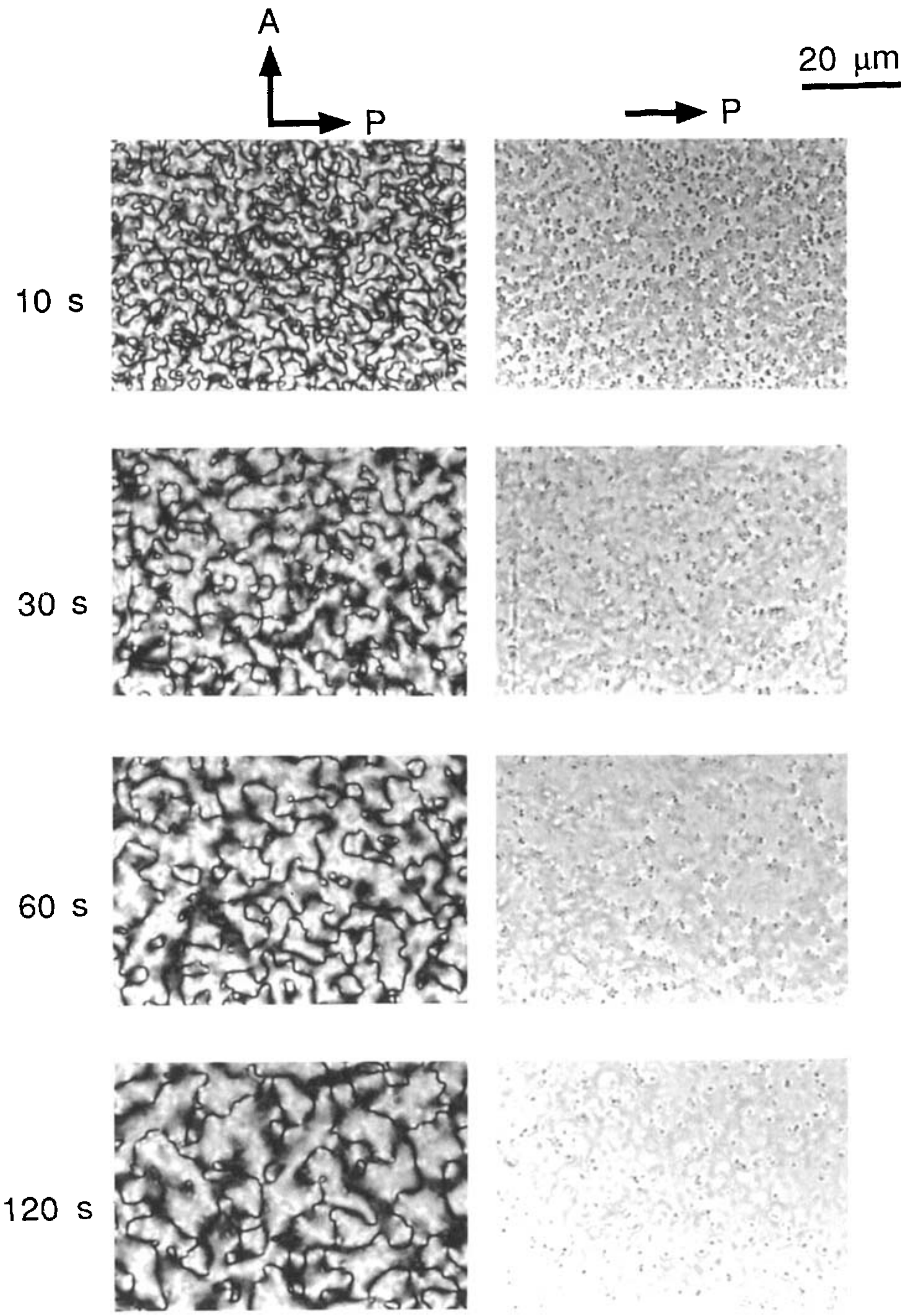

Figure 2. Variations of optical texture (left) and of the corresponding number of disclinations (right) with annealing time at 240°C. The polarizer and analyser are indicated by the letters P and A, respectively.

the directors in textures such as those shown in figure 1 or 2 has been analysed qualitatively by Hashimoto *et al.* [7, 8], and quantitatively by Greco [20]. The scattering angle $\theta_m$ of the intensity maximum for the $H_V$ scattering is related to the domain size, $D(t)$, as defined in previous work [6],

$$D(t) = 2\pi/q_m(t) \tag{1}$$

where

$$q_m(t) = (4\pi/\lambda)\sin[\theta_m(t)/2] \tag{2}$$

and $\lambda$ is the wavelength of light in the medium. Thus the

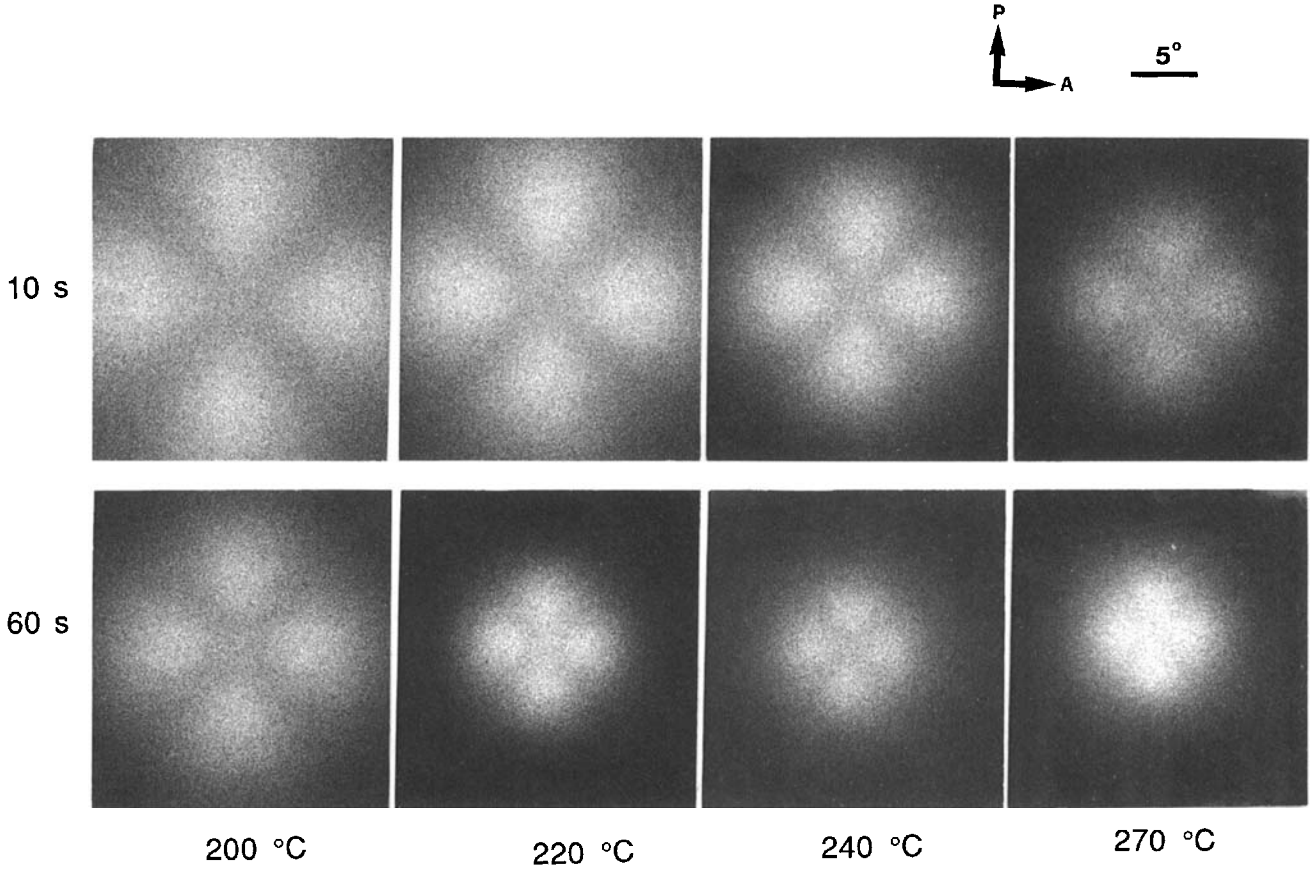

Figure 3. $H_V$ scattering patterns of the liquid crystal phase of X-7G obtained within a test temperature range of 200–270°C at two annealing times of 10 and 60 s. The orientation of the crossed polarizers (P and A) is indicated.

shift of $\theta_m$ or $q_m$ towards smaller values corresponds to growth of $D(t)$ or a decrease in the number density of disclinations. The results indicate that $D$ increases with $t$ and that $D(t)$ depends on the annealing temperature.

The influences of annealing temperature and time on the average distance between disclinations were determined from the micrographs, some of which are shown in figures 1 and 2, or from the scattering patterns, some of which are shown in figure 3. The results are shown in figure 4 of which 4(*a*) was determined from optical microscopy (OM) and 4(*b*) from light scattering (LS). $D(t)$ was determined microscopically from $\rho(t)$

$$D(t) = 1/[\rho(t)]^{1/2} \tag{3}$$

where $\rho(t)$ is the disclination density directly determined from the micrographs in figure 4(*a*). The size of liquid crystalline domain, $D$, was also determined from the LS patterns according to equations (1) and (2). Within $t < 100$ s, the time evolution of $D$ approximately obeys a power law with the exponent of *c*. 0·35, i.e.

$$D(t) \sim t^{0\cdot35} \tag{4}$$

except for the data obtained at 200°C (at $10 < t < 100$ s). The result given in equation (4) is consistent with our previous results obtained at 240°C [6], indicating again that our experimental result can be reproduced very well.

On the basis of the time-dependent Ginzburg–Landau model with non-conserved order parameter and assuming that defects are topologically point-like and that the attractive force between them is given by $r^{-1}$, where $r$ is the separation between the two defects, Toyoki [14] obtained a scaling relation of $D(t) \sim t^{1/2}$ in two-dimensional space. Clearly, the exponent obtained in our experiment is smaller than 1/2. In another case Rieger [15] proposed a mean field theory in the context of a diffusion-reaction model of the type $A + B \rightarrow 0$, where $A$ and $B$ correspond to the two disclinations with opposite sign. He obtained a non-power law relation between $\rho$ and $t$ given by

$$-\frac{a + b \ln \rho}{\rho} + c = t \tag{5}$$

where $a$, $b$ and $c$ are phenomenological constants. As Rieger pointed out, our data at $10 < t < 100$ s in figure 4 can be fitted well by equation (5): the non-power law behaviour suggested by Rieger also seems to be consistent

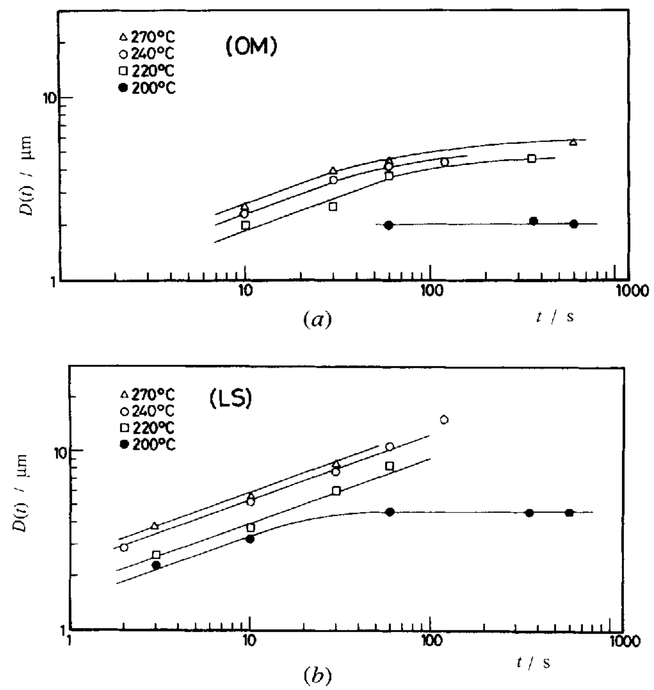

(a)

(b)

Figure 4. The logarithmic plots of the square root of the average area per disclination, D, determined by microscopy (*a*) and the size of liquid crystalline domain, D, determined by the scattering method (*b*) versus isothermal annealing time *t*, at 200, 220, 240 and 270°C.

with the annihilation kinetics found in our experiments. It is not possible to differentiate between the two different time dependences in the narrow time range covered in our experiments. Finally it is interesting to note that the computer simulation results obtained by Hudson and Thomas [21] are also in agreement with our experimental results, showing the power law with an exponent of 0·35.

At $t > 100$ s, the domain size is so large that it is difficult to determine the values $\theta_m$ or $q_m$, and hence $D(t)$ precisely from the scattering patterns. However, it is straightforward to determine the size from microscopy. The growth rate determined from microscopy clearly shows a levelling off at $t > 100$ s. The following two factors are probably responsible for the levelling off. In the X-7G film specimens with a thickness smaller than 10 μm, we observed mainly wedge disclination lines with $s = \pm 1/2$. The free energy of the system is proportional to the number and hence the length of disclination lines. The excess free energy is relaxed by annihilation of the disclination lines through diffusion and coalescence processes. In the initial stage, some disclination lines may be suspended free in the specimen, while others may be anchored at the glass surface. The free disclination lines may be more mobile than the anchored ones. Annihilation can occur between the free disclination lines or between free and anchored disclination lines. With an increase of annealing time, the number of free disclination lines gradually decreases. The annihilation rate is slowed down first and finally is completely pinned, because only the anchored disclination line may exist in the late stages. Another factor is that the prolonged annealing may promote crystallization of some short OBA sequences. The melting point of crystals of pure polyOBA is higher than 300°C [17]. The crystallization may also restrict the motion of disclinations for further annihilation. Owing to these pinning effects, it is difficult to study the kinetics of annihilation process at $t > 100$ s.

At 200°C, we cannot detect the texture growth at $t \geq 60$ s (see figure 4 (*a*), i.e. the texture remains at the stage shown in the top two micrographs of figure 1, due to the pinning effect arising primarily from the crystallization. At 170°C, we observed that the isotropic film specimen transformed into an anisotropic film within a few seconds. However, the texture did not vary with time due to the pinning as a consequence of the crystallization. Below 170°C, the isotropic sample appears to be incapable of change due to vitrification. The glass transition temperatures, $T_g$, of X-7G are *c*. 120°C for the PET sequence and *c*. 170°C for the OBA sequence, as reported in the literature [16, 22] and also as determined by differential scanning calorimeter (DSC) in our other work [23]. This indicates that our X-7G film specimen can transform from an isotropic glassy state to liquid crystalline state upon isothermal annealing at a temperature higher than its $T_g$.

### 3.2. *Disclinations appearing in the copolyester*

The micrographs in figure 5 are three polarizing light micrographs obtained with crossed polarizers set at different orientations for a sample annealed at 270°C for 60 s and then frozen-in in a glassy state. Two disclinations with $s = +1$, as well as two disclinations with $s = +1/2$ and $s = -1/2$ are pointed out in figure 5. The strength of the disclination is determined by the number, $N$, of dark brushes around a single disclination, i.e. $|s| = N/4$. The sign is determined by the rotation direction of the brushes when the crossed polarizers are rotated, i.e for a positive disclination, the rotation direction of the brushes is the same as that of the crossed polarizers, while for a negative disclination it is opposite to that of the crossed polarizers. Our observations indicate that (i) disclinations with strength $s = \pm 1/2$ occur most frequently in the X-7G liquid crystalline specimens, as shown by the disclinations with two dark brushes in figures 1 and 2; (ii) a few disclinations occur with strength $s = +1$ as shown in figure 5; (iii) disclinations with strength $s = -1$ are observed on rare occasion. The results (i) to (iii) were also found in previous work [7, 8] and for a lyotropic liquid crystal formed from a soluble polydiacetylene in chloroform [12, 13]. These phenomena may be understood for

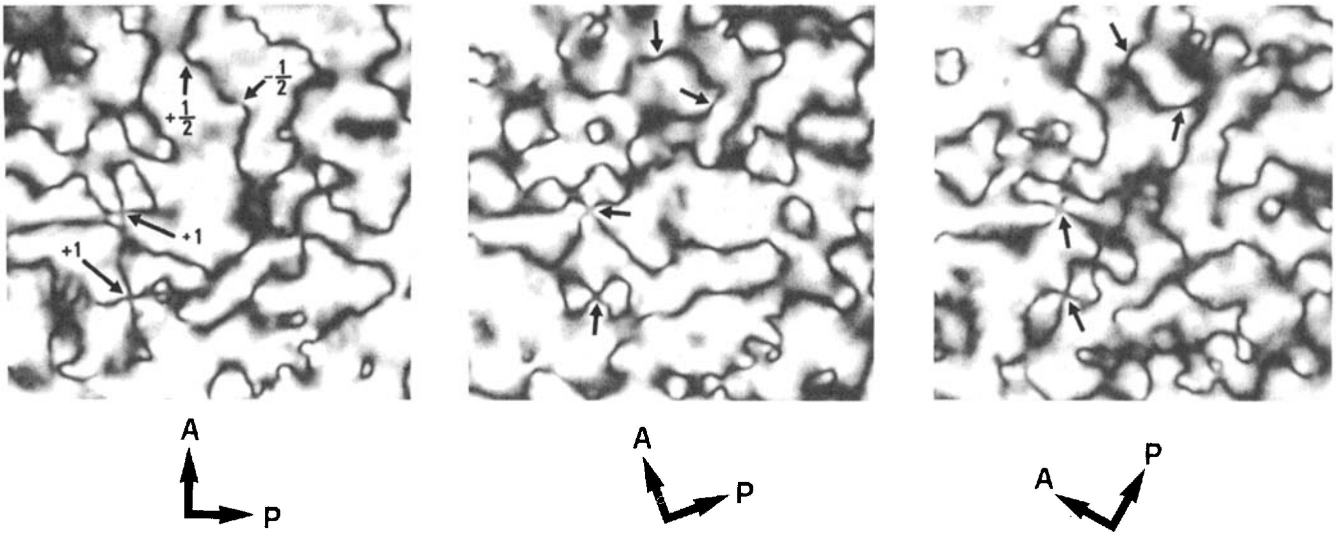

Figure 5. Two $s = +1$ disclinations and two $s = \pm 1/2$ disclinations which appeared in a film specimen of X-7G annealed at 270°C for 60 s. Their strength and sign were determined by the number of dark brushes and the rotation direction of the brushes when the crossed polarizers were rotated, as indicated. See also the text.

the following three reasons. (1) The disclination with $s = -1$ involves a very high deformation energy in rigid or semi-rigid macromolecules [12, 13]. (2) The free energy of an isolated $s = \pm 1$ disclination is higher than that of an isolated $s = \pm 1/2$ disclination. In the case of one constant approximation, i.e. that the splay elastic constant $k_{11}$ is equal to the bend elastic constant $k_{33}$, this free energy is proportional to $s^2$. (3) The interaction between the integer disclinations or that between the integer and half-integer disclinations is stronger than that between the half-integer disclinations. Therefore the $s = \pm 1$ disclinations should annihilate much faster than the $s = \pm 1/2$ disclinations.

At this stage it may be appropriate to compare our results with those obtained by Viney and Windle [18, 19], since the same LC copolyester was used. From the 10 μm thick slices prepared by microtoming as-received materials, Viney and Windle observed the schlieren textures on a much finer scale in the same temperature range as that used here. The disclinations appeared in their specimens to have the strengths $s = \pm 1/2$ and $\pm 1$. It appears that the texture coarsening occurred very slowly in their experiments. These differences in the size of the texture and the coarsening rate observed by two groups are believed to originate from the difference in preparation methods of the specimens. Clearly, the specimens microtomed from the as-received materials still maintain some kinds of structure built up when the as-received pellets were processed. This structure memory is very difficult to erase as the clearing temperature of X-7G is very high and close to its degradation temperature. The memory effect may strongly affect ordering processes or coarsening of the texture upon further annealing the specimens in the temperature range between 200 and 270°C. This is especially the case when crystallites composed of sequences rich in OBA or PET exist, because the crystallites suppress translational diffusion of X-7G molecules and hence the diffusion-coalescence of the defects necessary for the annihilation process.

### 3.3. *Annihilation microprocess*

Hereafter we define an annihilation process of a pair of disclinations as the *microprocess of annihilation*. In this section we focus on the dynamics of this microprocess. The micrographs in figure 6 were taken from the same area of the same sample at 240°C by OM with only one polarizer (see figure 6(*a*)) and with crossed polarizers (see figure 6(*b*)). They show the microprocess of annihilation of a pair of disclinations with $s = \pm 1/2$, as pointed out by the arrows 1 and 2 on the micrograph taken at 52 s after the *T*-jump (see figure 6 (*a*)) and a corresponding variation of the optical texture (see figure 6(*b*)) with time. According to the method used in figure 5, the sign and strength of disclinations appearing on the micrographs taken at $90 < t < 95$ s were determined from the following two micrographs, i.e. the one taken at 90 s with the orientation of the crossed polarizers as indicated in figure 6(*b*) and the other taken at $t = 95$ s with the orientation of the crossed polarizers rotated anticlockwise by 20° (not shown in figure 6). Figure 7 indicates the spatial distribution of disclinations so analysed at the time interval of $90 < t < 95$ s.

With increase of annealing time, the distance between the pair of the disclinations with $s = \pm 1/2$ decreases and then they coalesce to form a somewhat large dark spot as pointed out by an arrow on the micrograph taken at 101 s

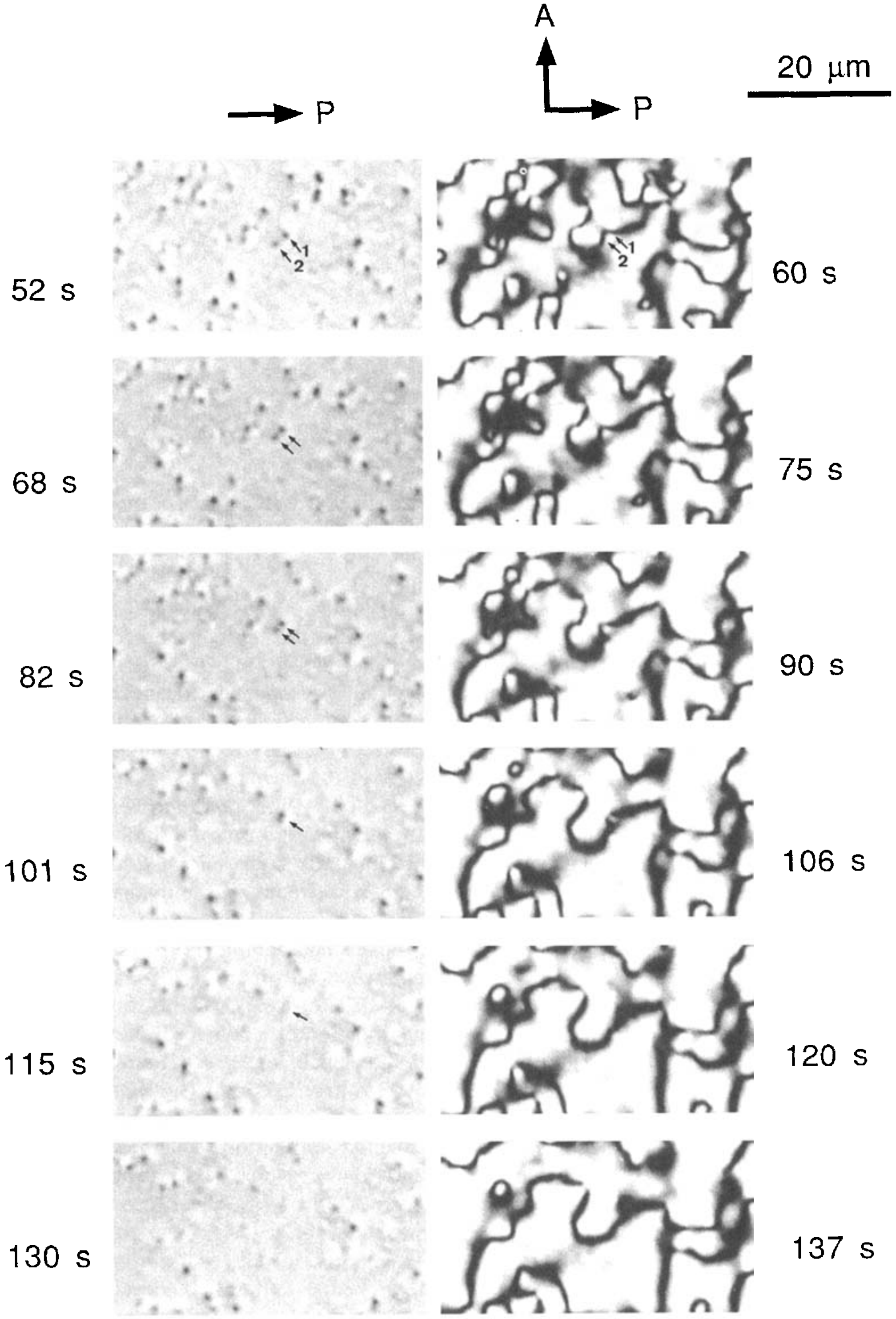

Figure 6. Optical micrographs taken during isothermal annealing at 240°C, showing (*a*) the annihilation microprocess of a pair of $s = \pm 1/2$ disclinations, as pointed out by arrows 1 and 2, respectively, and (*b*) the corresponding variation of the optical texture with time as seen through the microscope, with crossed polarizers. All the micrographs were obtained from the same area.

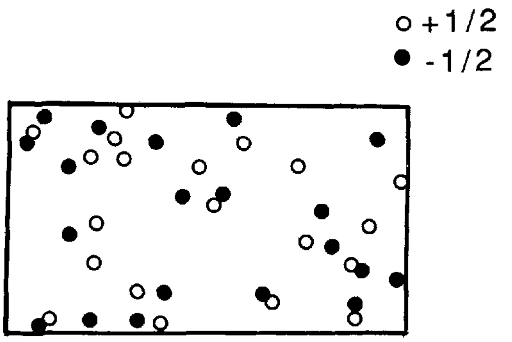

Figure 7. Spatial distribution of strength and sign of disclinations at the time interval of $90 < t < 95$ s in the experiment referred to in figure 6.

in figure 6. Finally they disappear from view at $101 < t < 115$ s. The annihilation microprocess of a pair of disclinations with $s = \pm 1/2$ is schematically represented in figure 8. Owing to the attractive interaction between the pair of disclinations with $s = \pm 1/2$, the distance between them gradually decreases (see figure 8 (*a*) and (*b*)) and they eventually annihilate (see figure 8 (*c*)). During this process, the molecules within the area between the two disclinations are gradually squeezed out, causing a continuous change of the director in such a way that the director trajectory is straightened along the direction in the area outside the pair of disclinations (see figure 8 (*b*) and (*c*)). Finally a locally perfect orientation is attained after the annihilation of the two disclinations (see figure 8 (*c*)). The corresponding variation of the schlieren texture is also shown in the figure. It should be noted that figure 8 schematically shows just one special configuration between the pair of disclinations with $s = \pm 1/2$. This configuration emphasizes splay deformation between the pair of disclinations. There is another configuration which emphasizes bend deformation between the pair of disclinations [2].

The micrographs in figure 9 were taken from the same area of the same sample at 240°C under the same conditions as those used in figure 6. They show the microprocess of annihilation of an $s = -1/2$ disclination and an $s = +1$ disclination, as pointed out by the arrows 3 and 4, respectively, on the micrograph taken at 68 s (see figure 9 (*a*)) and the corresponding variation of the optical texture (see figure 9 (*b*)) with time. The sign and strength of the disclinations were determined according to the method used in figure 5, and the sign and strength of the disclinations that appeared on the micrograph taken at the time interval of $90 < t < 95$ s are indicated in figure 10. Note that disclination 5 corresponds to the one with $s = -1/2$. The annihilation of the pair of disclinations formed by $s = +1$ and $s = -1/2$ in figure 9 results in the formation of a new disclination with $s = +1/2$ as pointed out by an arrow on the micrograph taken at $t = 145$ s. The microprocess of annihilation and the corresponding variation of the schlieren texture are schematically represented in figure 11. Owing to the attractive interaction between the pair of the disclinations with $s = -1/2$ and $+1$ ($c_0 = \pi/2$), the distance between them gradually decreases (see figure 11 (*a*) and (*b*)) and they eventually annihilate to form a new disclination with $s = +1/2$ (see figure 11 (*c*)). During this process the molecules in the

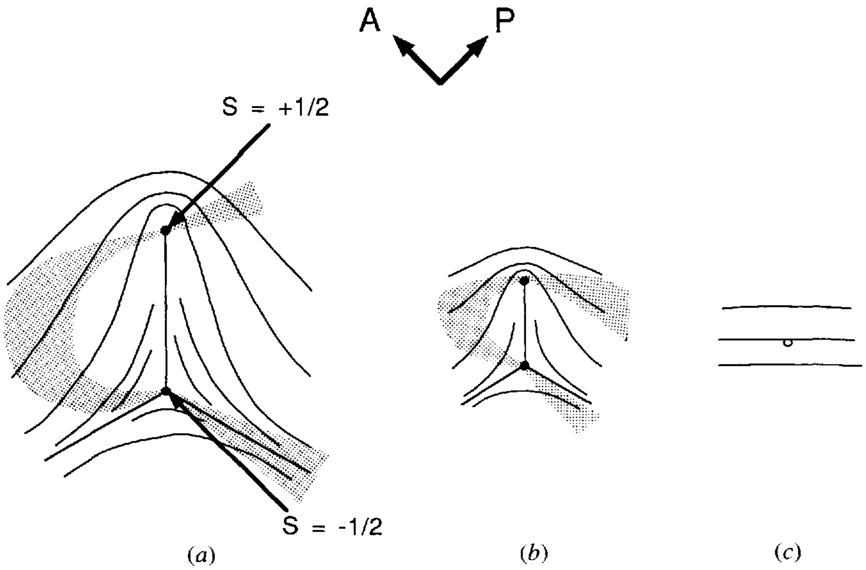

Figure 8. Schematic representation of the annihilation microprocess of a pair of $s = \pm 1/2$ disclinations and the corresponding variation of the schlieren texture with time.

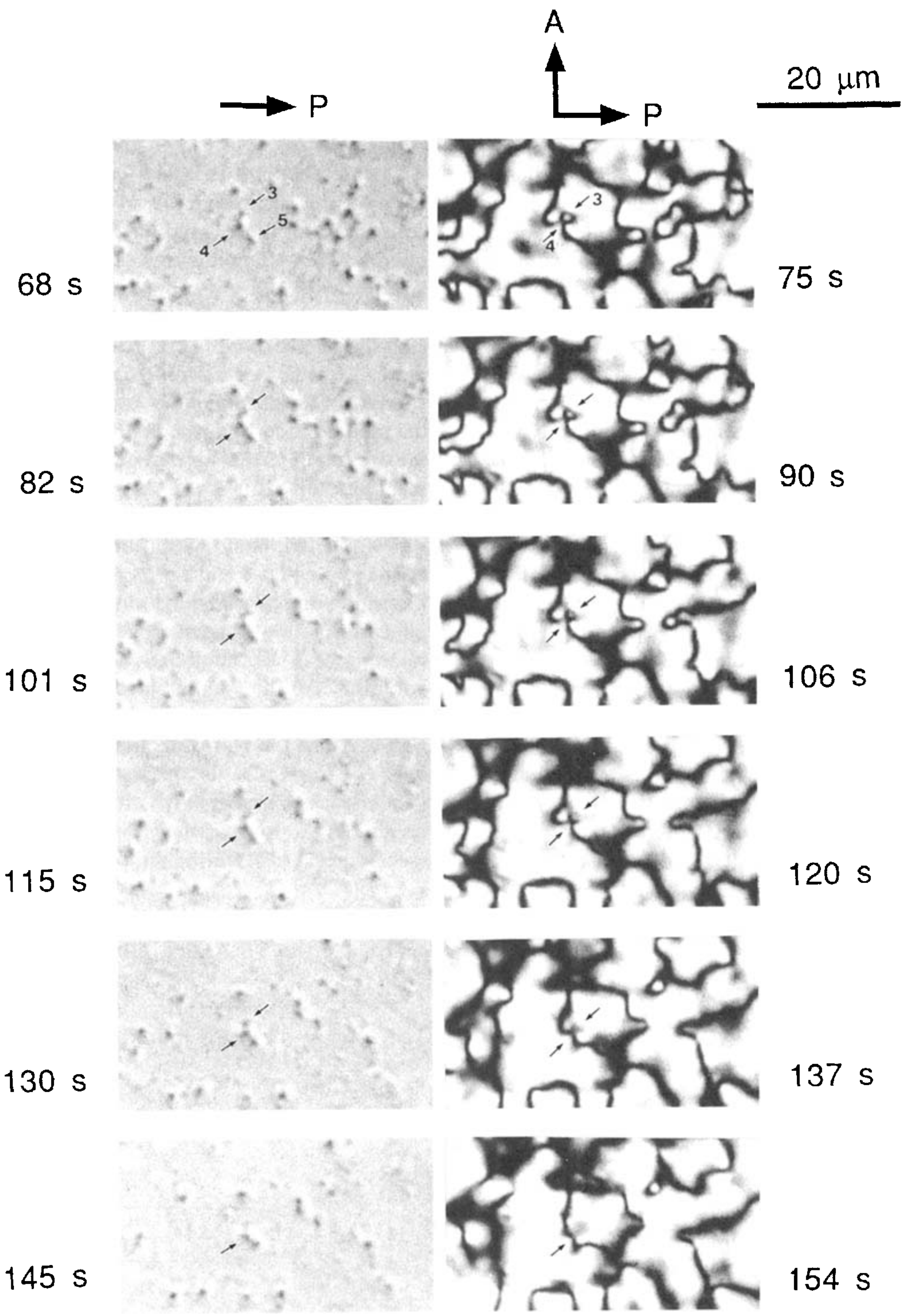

(*a*) (*b*)

Figure 9. Optical micrographs taken during isothermal annealing at 240°C, showing (*a*) the annihilation microprocess of a pair of disclinations with $s = -1/2$ and $+1$, as pointed out by arrows 3 and 4, respectively, and (*b*) the corresponding variation of the optical texture with time as seen through the microscope with crossed polarizers. All the micrographs were obtained from the same area. The disclination numbered 5 has $s = -1/2$.

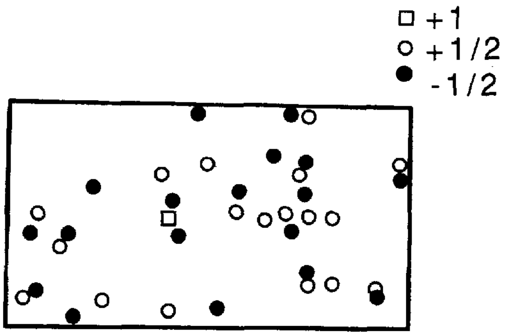

Figure 10. Spatial distribution of strength and sign of disclinations at the time interval of $90 < t < 95$ s in the experiment referred to in figure 9.

area between the two disclinations are gradually squeezed out (see figure 11 (*a*) and (*b*)). The director is continuously changed to an orientation suitable to the new disclination with $s = +1/2$ (see figure 11 (*c*)). It should be emphasized also that figure 11 is a schematic representation of just one possible microprocess of annihilation of the pair of disclinations with $s = -1/2$ and $+1$. In figure 11 we assume $c_0 = \pi/2$ for the disclinations with $s = +1$, but in this study we do not know which configuration the disclination with $s = +1$ has. It is important to note that the results discussed above indicate that the annihilation of opposite disclinations leads to coarsening of the schlieren texture as shown in figures 6 (*b*) and 9 (*b*).

The time variation of the distance, $r$, between the pairs of disclinations with opposite sign, as represented in figures 6 and 9, is shown in figure 12. For the pair of $s = \pm 1/2$ disclinations, the distance, $r$, decreases approximately in a linear manner with a slope of $-2{\cdot}8 \times 10^{-2}\,\mu\text{m}\,\text{s}^{-1}$ over the scale length covered in this experiment and finally approaches zero at $t \approx 115$ s, at which time the two disclinations annihilate and disappear from view (see figure 12 (*a*)). For the pair of disclinations with $s = -1/2$ and $+1$, the distance also decreases approximately in a linear manner with a slope of $-1{\cdot}2 \times 10^{-2}\,\mu\text{m}\,\text{s}^{-1}$ over the scale length covered in this experiment. They coalesce at $t \approx 145$ s, giving rise to a new disclination with $s = +1/2$, as shown in figure 9. At $t = 145$ s, $r \cong 1{\cdot}0\,\mu$m, a value which approximates closely to the size of the $s = +1/2$ disclination formed after annihilation of the pair of disclinations with $s = -1/2$ and $+1$. The dashed line in figure 12 (*a*) was obtained by plotting $(r(t) - 1{\cdot}0)\,\mu$m versus time, i.e. by vertically shifting the solid line of the data for the pair of $s = +1$ and $-1/2$ disclinations. The dashed line indicates a real variation of the distance during the annihilation microprocess. It reduces to zero at $t \cong 145$ s.

Many such microprocesses have been observed in this study. In the case of a relatively isolated pair of disclinations, the distance normally decreases in an approximately linear manner with annealing time, but the slope, and therefore the velocity of disclination motion, is different from one to another; this is believed to be an effect of disclinations surrounding the particular pair of our interest. In a system with many disclinations, the force $\mathbf{F}_i$ acting on the $i$th disclination is

$$\mathbf{F}_i = 2\pi K s_i \sum_{j \neq i} s_j \frac{\mathbf{r}_i - \mathbf{r}_j}{|\mathbf{r}_i - \mathbf{r}_j|^2} \tag{6}$$

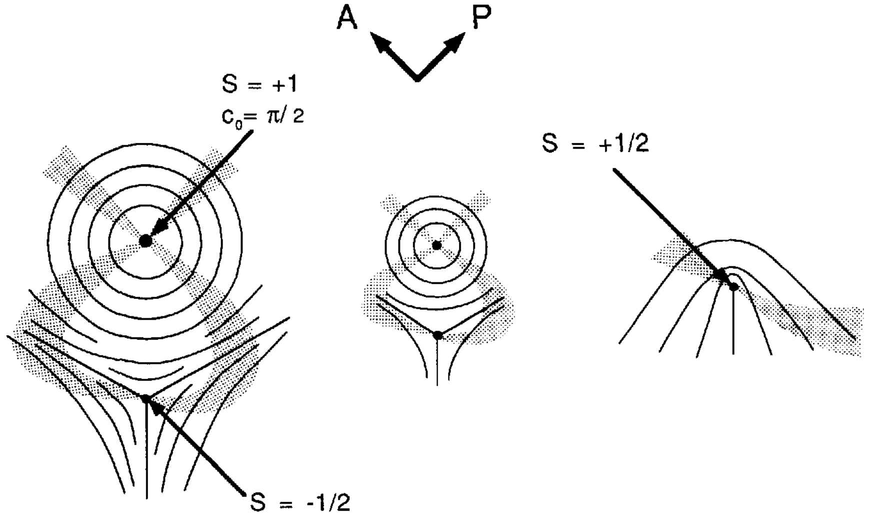

(*a*) (*b*) (*c*)

Figure 11. Schematic representation of the annihilation microprocess of a pair of disclinations with $s = -1/2$ and $+1$ and the corresponding variation of the schlieren texture with time.

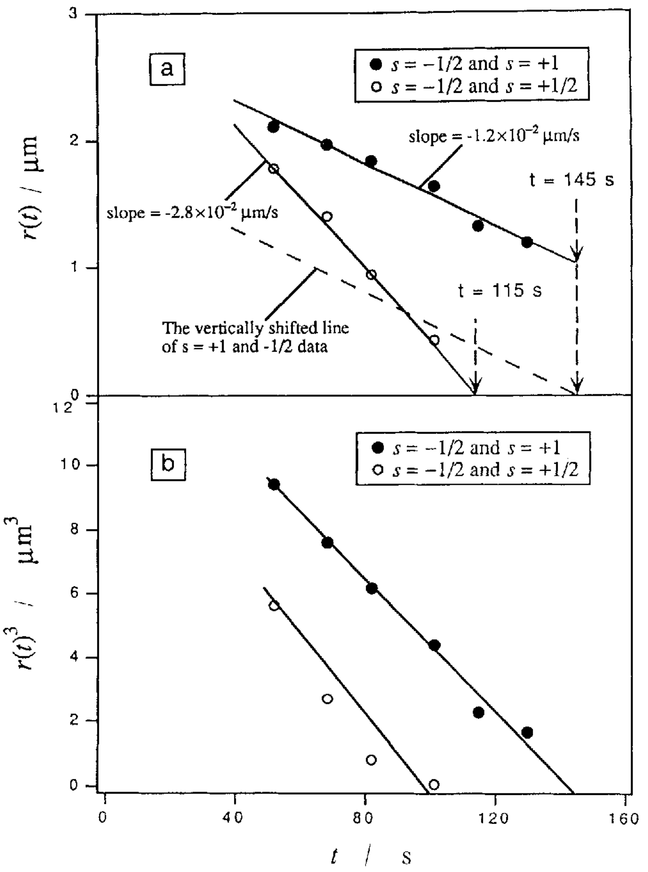

Figure 12. Plots of distance, $r$, between the pair of $s = -1/2$ and $+1/2$ disclinations and the pair of $s = -1/2$ and $+1$ disclination shown in figures 6 and 9, respectively, versus isothermal annealing time, $t$, at 240°C. (*a*) Plot of $r(t)$ versus $t$ and (*b*) plot of $r(t)^3$ versus $t$.

where $K$ is a Frank elastic constant ($K \equiv k_{33} = k_{11}$; $k_{11}$ being assumed to be equal to $k_{33}$) and $\mathbf{r}_i$ the position of the $i$th disclination [24]. The variation in the slope may indicate that the interaction between a pair of disclinations is affected more or less by surrounding disclinations. In figure 12 (*a*), the relatively small slope for the annihilation of $s = +1$ and $-1/2$ disclination does indicate that the interaction between the pair of disclinations is affected strongly by the neighbouring one with $s = -1/2$, which is pointed out by the arrow numbered 5 in figure 9.

It may be interesting to interrelate the data obtained on the annihilation microprocess ($r(t)$ in figure 12) and the data obtained on the ordering process of the systems containing many disclinations ($D(t)$ in figure 4). Let us consider the following scenario for a very qualitative analysis. The experiments on the annihilation microprocess may yield an average annihilation rate constant $k(t)$

$$k(t) \cong -\frac{\mathrm{d}r(t)}{\mathrm{d}t}\Big/ r(t). \qquad (7)$$

Knowing the rate constant $k(t)$, we may write the annihilation rate equation

$$-\frac{\mathrm{d}\rho(t)}{\mathrm{d}t} = k(t)\rho(t). \qquad (8)$$

The solution of this equation may then account for the experimental $D(t)$ data through equation (3). In $d$-dimensional space, equation (3) is written by

$$D(t) = \frac{1}{\rho(t)^{1/d}}. \qquad (9)$$

The data on $D(t)$ are thus related to the data on $\mathrm{d}r(t)/\mathrm{d}t$ obtained for the elementary microprocess.

The defect motion is so slow that the force acting on the defects may be approximated to by the static force and balances with the dissipative forces proportional to the velocity of the defects. Then we obtain the equation of defect motion,

$$\frac{\mathrm{d}\mathbf{r}_i}{\mathrm{d}t} \sim \mathbf{F}_i = 2\pi K s_i \sum_{j \neq i} s_j \frac{\mathbf{r}_i - \mathbf{r}_j}{|\mathbf{r}_i - \mathbf{r}_j|^{\beta+1}}. \qquad (10)$$

Here we generalize equation (6) by introducing an exponent $\beta$ on the force–distance relation for the sake of convenience. For the two-dimensional problem with $\beta = 1$, the r.h.s. of equation (10) for $\mathbf{F}_i$ reduces to equation (6). Applying equation (10) in the case of an isolated pair of defects of opposite sign with a separation distance $r(t)$, we obtain

$$\frac{\mathrm{d}r(t)}{\mathrm{d}t} \sim -r(t)^{-\beta}. \qquad (11)$$

The solution of equation (11) is given by

$$r(t)^{\beta+1} = at + b \qquad (12)$$

where $a$ and $b$ are constants.

From equations (7) and (11), we may approximately estimate the rate constant $k$,

$$k \cong r(t)^{-(\beta+1)}. \qquad (13)$$

From equations (8) and (13) and noting that $r(t) \sim \rho(t)^{-1/d}$,

$$-\frac{\mathrm{d}\rho(t)}{\mathrm{d}t} \sim \rho(t)^{(d+\beta-1)/d}. \qquad (14)$$

Equation (14) gives

$$\rho(t) \sim t^{-d/(\beta+1)} \qquad (15)$$

and

$$D(t) \sim t^{1/(\beta+1)}. \qquad (16)$$

In the case where $\beta = 1$, $D(t) \sim t^{1/2}$, of which the scaling law was predicted by Toyoki [14] and experimentally observed by Nagaya *et al.* [10]. However, we observed the different scaling law of equation (4), corresponding to the case of $\beta \cong 2$, instead of $\beta = 1$. The corresponding microprocess is then given by

$$r(t)^3 = at + b \tag{17}$$

so that $r(t)^3$ instead of $r(t)^2$ (the case of Nagaya *et al.*) should linearly decrease with $t$. Figure 12 (*b*) shows the plots of $r(t)^3$ versus $t$. The experimental results shown by filled and unfilled circles are consistent with the prediction given by equation (17) (straight lines). The physical interpretation of $\beta = 2$, instead of $\beta = 1$ observed for small molecular liquid crystals [10, 11], deserves future studies.

## 4. Summary

In this study we have shown that, within the test temperature range used, the annihilation kinetics of pairwise disclinations in the LC copolyester specimen can be divided into the following two stages. In the early stage ($t < 100$ s), the annihilation results in growth of the domain size $D$ approximately according to a power law of $D(t) \sim t^{0.35}$. The observed power law is consistent with the time-dependence proposed by Rieger [15] based on the diffusion-reaction model over the narrow time scale covered in this experiment. It is not possible to differentiate the two different time dependences at this moment. In the later stage ($t > 100$ s), anchoring of some of the disclination lines at the glass surface and/or formation of fine crystallites, composed of sequences rich in OBA or PET, in the copolyester first suppress and then pin the annihilation process. This leads to a slowing down of the growth rate of domains and to a break down of the power law.

The annihilation microprocesses between $s = +1/2$ and $s = -1/2$ or between $s = +1$ and $s = -1/2$ pairwise disclinations were directly observed *in situ* by optical microscopy. The results indicate that the distance $r$ between them decreases with time $t$ approximately in a linear manner, but the slope is different from one to another over the scale length covered in the experiment. The variations of the slope imply the importance of many body interactions: the pairwise interaction is strongly affected by surrounding defects. The results of $r(t)$ versus $t$ also fit with the picture leading to a linear decrease of $r(t)^3$ versus $t$, i.e. the picture consistent with $D(t) \sim t^{0.35}$. The annihilation between $s = \pm 1/2$ pairwise disclinations leads to a locally perfect orientation of molecules and hence the distance between them reduces to zero, whereas the annihilation between $s = +1$ and $s = -1/2$ pairwise disclinations gives rise to formation of a new disclination with $s = +1/2$ and the distance is approximately reduced to the core size of the new disclination.

## References

[1] Demus, D., and Richter, L., 1978, *Textures of Liquid Crystals* (Verlag Chemie, Weinheim).
[2] Chandrasekhar, S., and Ranganath, G. S., 1986, *Adv. Phys.*, **35,** 507.
[3] Kléman, M., 1989, *Rep. prog. Phys.*, **52,** 555 and 1989, *Liq. Crystals*, **5,** 399.
[4] Saupe, A., 1973, *Molec. Crystals liq. Crystals*, **21,** 211.
[5] Sonin, A. S., Chuvyrov, A. N., Sobachkin, A. A., and Ovchinnikov, V. L., 1976, *Soviet Phys. Sol. St.*, **18,** 1905.
[6] Shiwaku, T., Nakai, A., Hasegawa, H., and Hashimoto, T., 1987, *Polymer Commun.*, **28,** 174.
[7] Hashimoto, T., Nakai, A., Shiwaku, T., Hasegawa, H., Rojstaczer, S. R., and Stein, R. S., 1989, *Macromolecules*, **22,** 422.
[8] Shiwaku, T., Nakai, A., Hasegawa, H., and Hashimoto, T., 1990, *Macromolecules*, **23,** 1590.
[9] Rojstaczer, S. R., and Stein, R. S., 1990, *Macromolecules*, **23,** 4863.
[10] Nagaya, T., Hotta, H., Orihara, H., and Ishibashi, Y., 1991, *J. phys. Soc. Japan*, **60,** 1572.
[11] Nagaya, T., Hotta, H., Orihara, H., and Ishibashi, Y., 1992, *J. phys. Soc. Japan*, **61,** 3511.
[12] Wang, W., Lieser, G., and Wegner, G., 1993, *Liq. Crystals*, **15,** 1.
[13] Wang, W., 1993, Ph.D. thesis, University of Marburg, Marburg, Germany.
[14] Toyoki, H., 1990, *Phys. Rev. A*, **42,** 911.
[15] Rieger, J., 1990, *Macromolecules*, **23,** 1545.
[16] Jackson, W. J., and Kuhfuss, H. F., 1976, *J. Polym. Sci., Polym. Chem. Ed.*, **14,** 2043.
[17] McFarlane, F. E., Nicely, V. A., and Davis, T. G., 1979, *Contemporary Topics in Polymer Science*, edited by E. M. Pearce and J. R. Schafgen (Plenum), Vol. 2.
[18] Viney, C., and Windle, A. H., 1982, *J. mater. Sci.*, **17,** 2661.
[19] Windle, A. H., Viney, C., Golombok, R., Donald, A. M., and Mitchell, A. M., 1985, *Faraday Discuss. Chem. Soc.*, **79,** 55.
[20] Greco, F., 1989, *Macromolecules*, **22,** 4622.
[21] Hudson, S. D., and Thomas, E. L., 1991, *Chemtracts—Macromolecular Chem.*, **2,** 73.
[22] Meesiri, W., Menczel, J., Gaur, U., and Wunderlich, B., 1982, *J. Polym. Sci., Polym. Phys. Ed.*, **20,** 718.
[23] Nakai, A., Shiwaku, T., Wang, W., Hasegawa, H., and Hashimoto, T., *Polymer* (in the press).
[24] Nürgen, J., and Saupe, A., 1972, *J. chem. Soc., Faraday Trans. II*, **68,** 1.